Electronic Supplementary Material (ESI) for Journal of Materials Chemistry C.

Supporting information for

Greatly Enhanced Dielectric Charge Storage Capabilities of Layered Polymer Composites Incorporated with low loading fractions of Ultrathin Amorphous Iron Phosphate Nanosheets

Meiyu Zhang[a], Zhicheng Shi[a, *], Jifu Zhang[a], Kun Zhang[b], Li Lei[a], Davoud Dastan[c], Bohua Dong[a, *]

[a]School of Materials Science and Engineering, Ocean University of China, Qingdao 266100, P. R. China

[b]Key Laboratory of Microgravity (National Microgravity Laboratory), Institute of Mechanics, Chinese Academy of Sciences, Beijing 100190, China

[c]Department of Materials Science and Engineering, Georgia Institute of Technology, Atlanta, Georgia-30332, USA

[*]Corresponding author: E-mail: zcshi@ouc.edu.cn; dongbohua@ouc.edu.cn

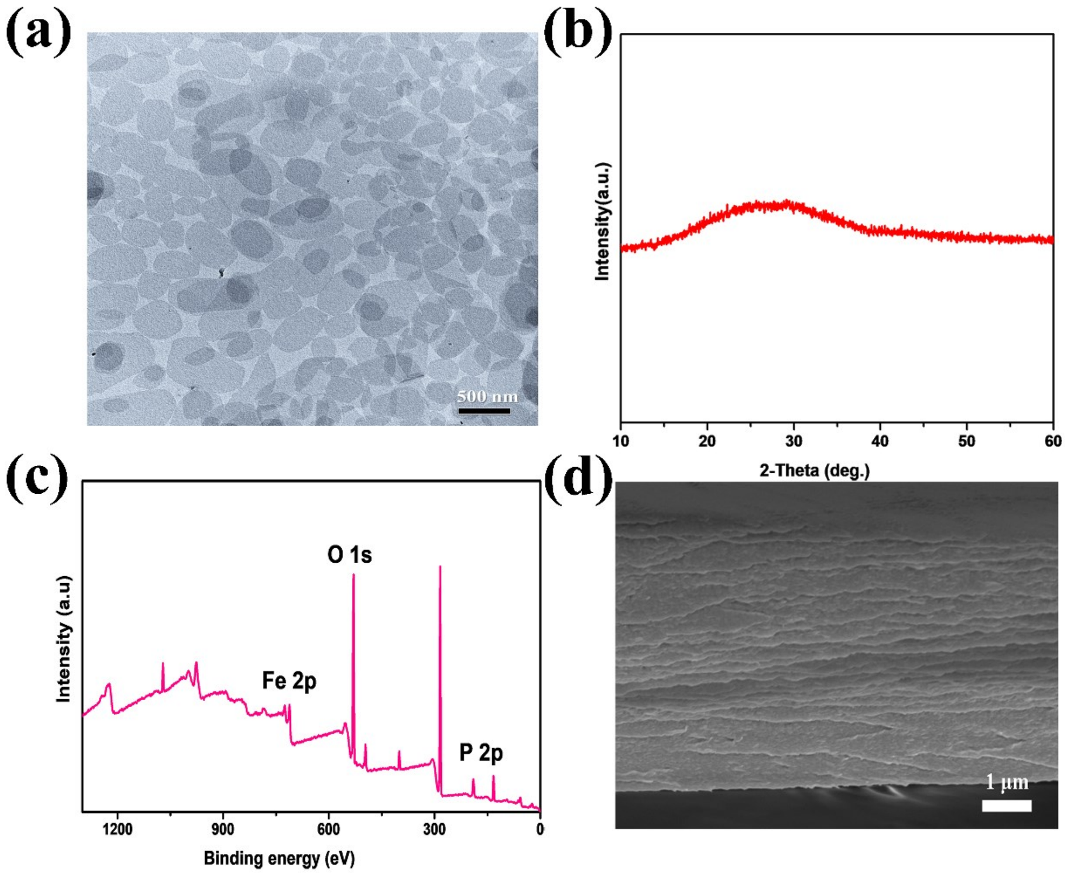

Fig. S1 (**a**) TEM images of amorphous $FePO_4$ nanosheets, (**b**) The wide-angle XRD pattern of amorphous $FePO_4$ nanosheets, (**c**) XPS spectrum of $FePO_4$ nanosheets showing the composition of both Fe, P and O, (**d**) Cross-sectional SEM morphology of PEI film.

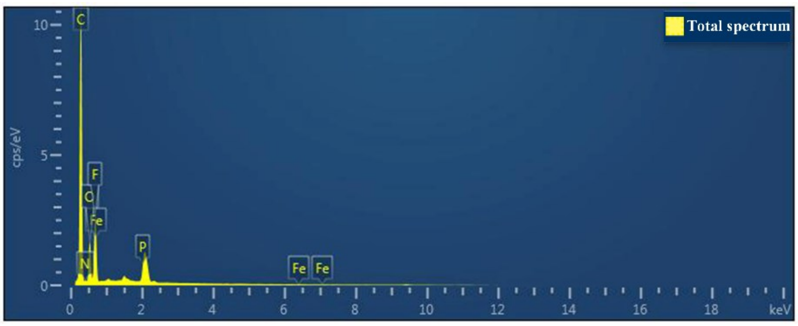

Fig. S2 Total spectrum

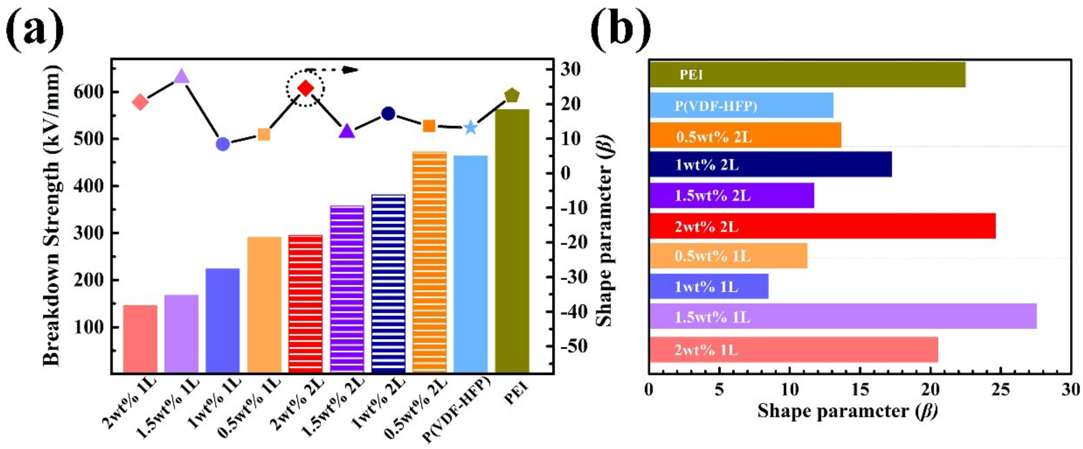

Fig. S3 (**a**) Comparison of the breakdown strength and shape parameters β of single-layer and bilayer composites with different $FePO_4$ mass fractions, (**b**) Horizontal comparison of the shape parameters β of single-layer and bilayer composites with different $FePO_4$ mass fractions.

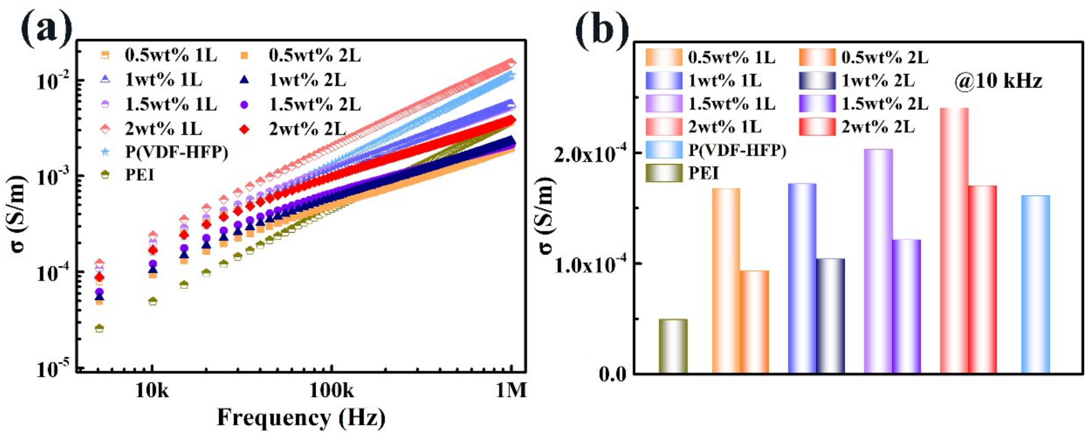

Fig. S4 (a) The frequency dependence of the electrical conductivity of single-layer and bilayer composites, (**b**) The electrical conductivity of single-layer and bilayer composites with different $FePO_4$ loading fractions.

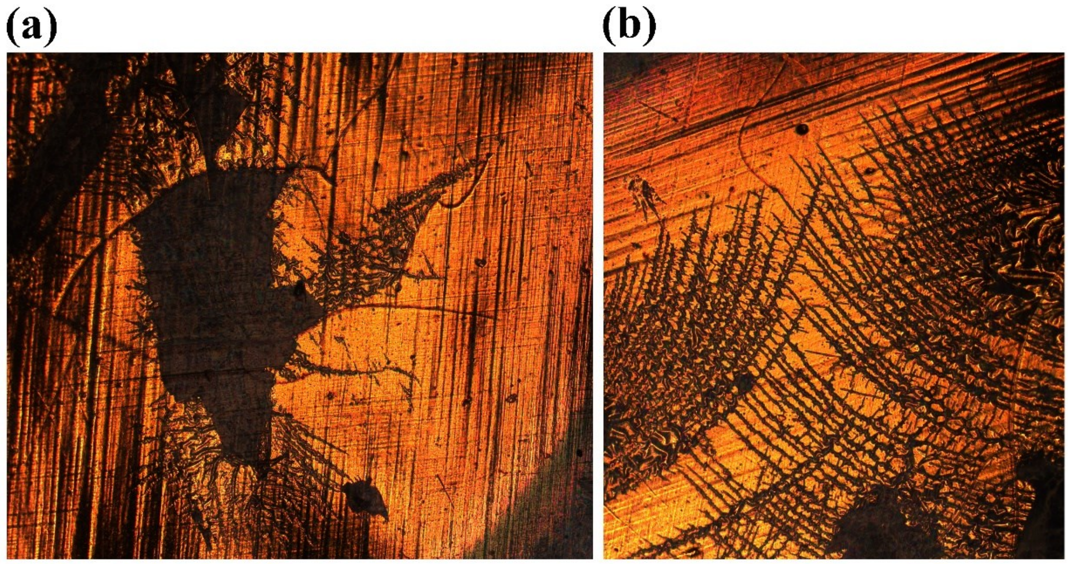

Fig. S5 Observe electrical tree branches (a) on the surface of the sample after breakdown under a metallographic microscope, (b) The picture shows a partial enlargement of the electrical tree.

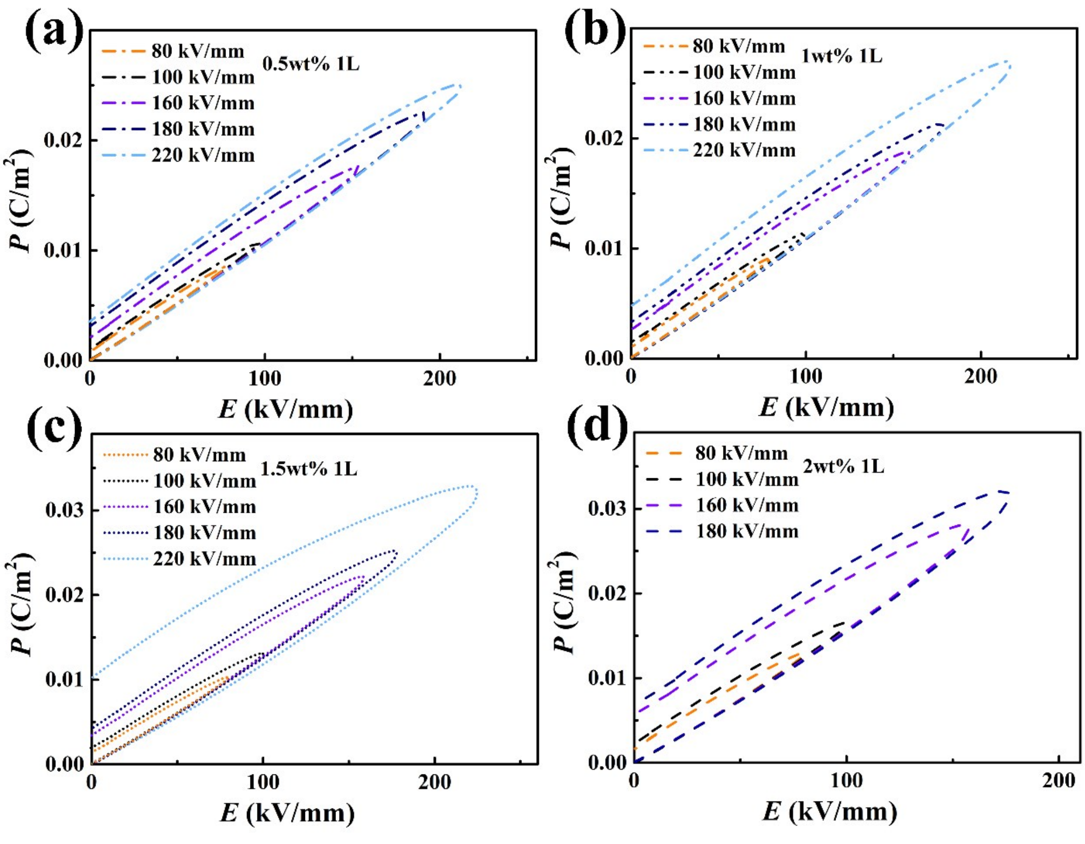

Fig. S6 *P*-*E* loops of $FePO_4$/P(VDF-HFP) single-layer films with different $FePO_4$ mass fraction ratios.

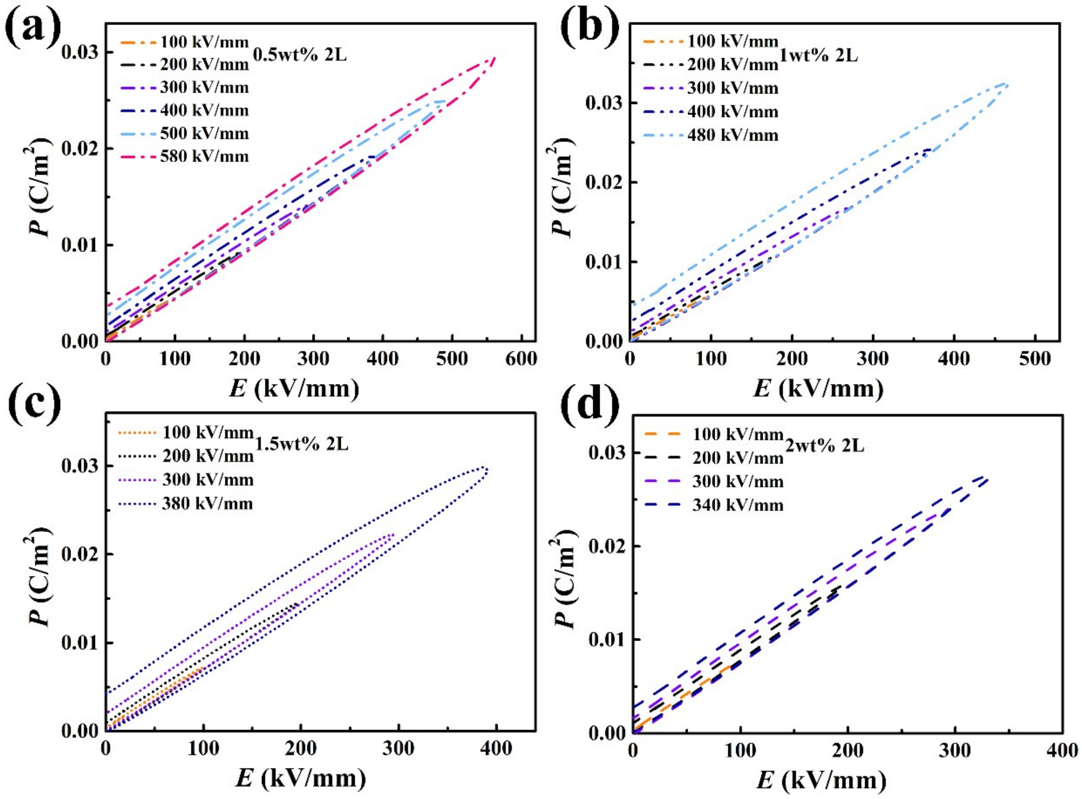

Fig. S7 *P*-*E* loops of $FePO_4$/P(VDF-HFP)-PEI bilayer films with different $FePO_4$ mass fraction ratios.

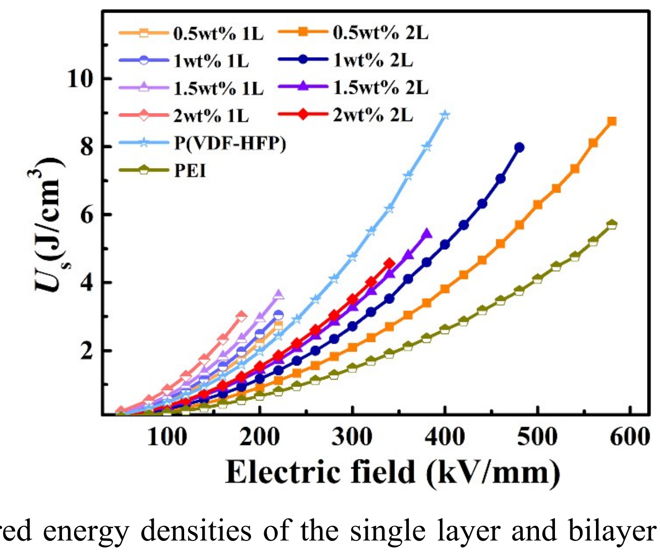

Fig. S8 The stored energy densities of the single layer and bilayer composites under varied external electric fields.

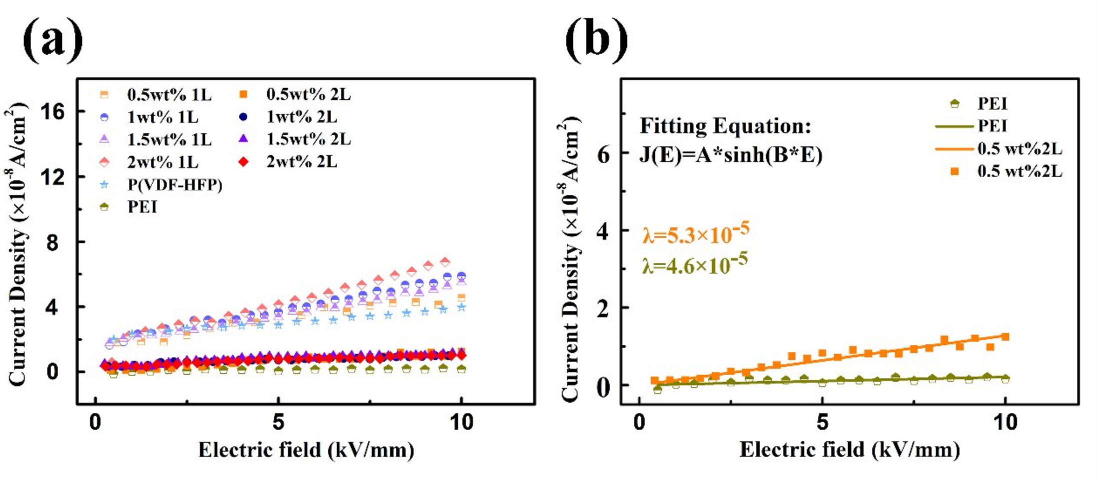

Fig. S9 (**a**)The variation of leakage current for 1L and 2L composite films with different filling fraction of $FePO_4$ nanosheets, (**b**) The leakage current density of PEI and 0.5 wt% 2L nanocomposite as a function of electric field at room temperature. The solid line represents the fit performed by the jump conduction equation.

The *J*-*E* curves are fitted using a hopping conduction model:[S1, S2]

$$J(E,T) = 2ne\lambda v * \exp(-W_a/K_B T) * \sinh(\lambda eE/2K_B T) \quad \text{(S1)}$$

where J is the leakage current, n is the carrier concentration, e is the charge of the carriers, λ is the hopping distance, v is the attempt-to-escape frequency, W_a is the activation energy, and K_B is the Boltzmann constant. At a fixed temperature, equation (S1) can be simplified as:

$$J(E) = A * \sinh(B * E) \quad \text{(S2)}$$

where A and B are two lumped parameters. The fitted results are shown in **Fig. S9**.

References

S1 H. Li, D. Ai, L. L. Ren, B. Yao, Z. B. Han, Z. H. Shen, J. J. Wang, L. Q. Chen and Q. Wang, Adv. Mater., 2019, **31**, 1900875.

S2 L. L. Ren, H. Li, Z. L. Xie, D. Ai, Y. Zhou, Y. Liu, S. Y. Zhang, L. J. Yang, X. T. Zhao, Z. R. Peng, R. J. Liao and Q. Wang, Adv. Energy Mater., 2021, https://doi.org/10.1002/aenm.202101297.